SINERGI Vol. 26, No. 1, February 2022: 91-98
http://publikasi.mercubuana.ac.id/index.php/sinergi
http://doi.org/10.22441/sinergi.2022.1.012

Computational investigation of various wedges electromagnetic wave absorbers on anechoic chambers

Naufal Baihaqi Al Afkar
Department of Mechanical Engineering, Universitas Negeri Semarang, Indonesia

Abstract
The anechoic chamber is closely related as a device for precisely measuring various acoustic characteristics. Anechoic chambers room conditions controlled to produce a sound field-free space. This study focused on testing various commercial wedges such as Eckel, diamond, pyramidal, and oblique pyramidal. The test was done by varying the elevation of an incident angle at 0°-85° with a stepping distance is 5°. This study is analyzed at 1-3 GHz frequency. This research was conducted based on a computational analysis using the finite element method on electromagnetic wave physics interfaces using COMSOL Multiphysics. The results show that, in general, pyramidal has the best performance. These results are assessed from the stability of absorption performance, the Eckel model obtains -66.6 dB at 1 GHz frequency but on another frequency tests with drastic performance fluctuations. In general, a pyramidal model can be an ideal absorber for anechoic applications because it provides good absorption performance for near normal and normal incidence angles. The results of the design and testing of the wedges model for anechoic are expected to be references in designing the optimal anechoic chamber room. Furthermore, it can contribute positively to tuning acoustic instruments such as microphones or reducing the antenna measurement error.

Keywords:
Anechoic Chamber;
Electromagnetic wave;
Finite element method;
Sound absorption;

Article History:
Received: June 22, 2021
Revised: August 4, 2021
Accepted: August 17, 2021
Published: February 1, 2022

Corresponding Author:
Naufal Baihaqi Al Afkar,
Department of Mechanical Engineering, Universitas Negeri Semarang, Indonesia
Email:
baihaqinaufal18@gmail.com

INTRODUCTION

Anechoic chambers are rooms that are designed to absorb all sound waves and produce a room environment without echoes and reverberation. This standard condition can be created if there is no reflection of sound waves from the floor, walls, and ceiling so that a room with free acoustic field conditions will be created. The design of the absorption layer on the anechoic chamber can absorb 99% of sound waves [1]. The sound produced in this room is lower echo and focused, and noise from the outdoor room can be perfectly muffled. This is the reason Anechoic chambers are very suitable for testing and calibration of acoustic instruments. Firmanto *et al.* [2] tested the recording of the speech sound database in a hemi-anechoic room for the development of an acoustic-phonetic approach system, the results of the study obtained a database of Indonesian people's regional accents. Not only damping stability in sound instrument testing but also in signal instrumentation testing, Sheret *et al* [3] measured the performance of the Antenna Under Test (AUT) aspects of amplification and signal characteristic patterns in the anechoic chamber with the interior layer coated with Radar Absorbent. Materials (RAM). Wiles and Kriz [4] also conducted antenna performance measurements, looking for value Normalized Signal Amplitude Deviation (NSA) and Free Space NSA (FSNA) with a variety of value measurement frequencies below 1 GHz and above 1 GHz as well as variations in the polarization direction signal, The test is done on Electromagnetic Compatibility (EMC) Fully Anechoic Rooms.

In general, anechoic chambers are classified into two types, the fully anechoic chamber and hemi anechoic chamber. Fully anechoic chambers are those chambers that are found on all sides of the room, such as the floors, ceilings, and walls. They are fully covered with sound-absorbing material from all directions. Meanwhile, in the hemi anechoic chamber, there is one side that is not covered with wave-absorbing material, generally the floor. The performance of the anechoic chamber cannot be separated from the sound wave absorbing material known as wedges. A wide frequency range setting is required with a thin wedges thickness, so the result of reflection will be lower [5] it also provides a high precision to the sound of acoustic measurement.

The standard design of using wedges in the anechoic chamber is required to provide a sound energy absorption performance of at least 99% following the ISO 3745 (2003) standard [6]. Within the given frequency range, the usual incoming sound energy absorption coefficient of walls, floors, and ceilings must be more significant than 99%, with the cut-off frequency being the lowest value of this requirement. The theoretical calculation of the cut-off frequency needs to be carried out before the process of making the anechoic chamber, especially on the wedges section, the calculation results are used to determine the specifications for the desired frequency range capability.

$$f = \frac{c}{4L} \quad (1)$$

The most frequently recognized theoretical formula for finding a room's cut-off frequency is shown in Equation 1, where f is the cut-off frequency, c is the sound speed (343.3 m/s), and L is the length of the wedges utilized.

Sound waves can propagate directly from the source to the receiver in free field conditions [7]. When a sound wave hits the end of a medium or comes over an impediment in its route, it performs a behavior known as boundary behavior. Conducts that may occur include reflection, diffraction, transmission, and diffusion. The phenomenon of echo or reverberation can occur due to the reflection of sound waves on the surface of the medium, the amount of reflection depends on the dissimilarity of the two mediums (i.e. air with polyurethane foams). Unobstructed sound can be created when the wave is not affected much by behaviors such as reflection, absorption, deflection, diffraction, refraction, diffusion and is not affected by the effects of resonance [8]. Literature studies conducted by many researchers state that the selection of the medium material and the shape of the wedges significantly affect the absorption performance to produce a space without echo [9, 10, 11].

The perfect free-reflection of sound in anechoic chamber design provides precise measurement of noise source sound power levels, this condition is also ideal for calibrating electro-acoustic measuring instruments and measuring the performance of various electro-acoustic products [12, 13, 14]. To obtain better anechoic room performance, it is necessary to have a special study related to determining factors such as type of materials, shapes, and the effects of the distance and angle of incidence of waves. Parameters that have a positive effect can be known through observation of the differences in the test results from various parameters.

This paper discusses the effect of using the shape of the wedges anechoic chamber with variations in the workspace frequency. The finite element method (FEM) is used to create the behavior condition of the wedges. FEM is a numerical method with a simple concept that divides complex problems into small parts called meshes to make it easier to find equation solutions and then combine each solution to solve complex problems [15]. The computational investigation was carried out using COMSOL Multiphysics Software, the electromagnetic waves physics interfaces feature completed the simulation.

METHODS

Reflection And Transmission of Electromagnetic Waves

Sound waves are pressure disturbances that move in a medium through interactions between particles. In a free field condition, the waves from the sound source can propagate freely from the air medium to reach another medium. Some of the waves will be reflected, and others will be transmitted across the boundary, the direction and condition of the wave reflection become one of the biggest factors causing the occurrence of echo. Figure 1 shows the oblique incident at the dielectric boundary of the plane, where sections I, II and III are incident waves, reflected waves, and refracted waves. The medium I assume to be free space (air) with magnetic permeability μ_1 and dielectric permittivity ε_1, while medium II is a solid material (assuming value z>0) with magnetic permeability μ_2 and dielectric permittivity ε_2.

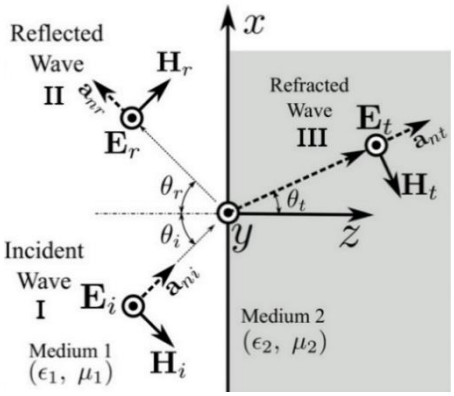

Figure 1. Oblique Incidence at a plane Dielectric Boundary Perpendicular Polarized

For a perpendicular polarized plane electromagnetic wave, the incident and reflected fields are as follows:

$$\begin{aligned}\mathrm{E}_1 &= a_y\left[E_{0i}e^{-j\beta_1(z\cos\theta_i+x\sin\theta_i)}\right. \\ &+ \left. E_{0r}e^{-j\beta_1(-z\cos\theta_r+x\sin\theta_r)}\right]\end{aligned} \quad (2)$$

$$\mathrm{E}_2 = a_y E_{0t}e^{-j\beta_2(z\cos\theta_t+x\sin\theta_t)} \quad (3)$$

Incidence, reflection, and refraction angles are represented by θ_i, θ_r, and θ_t Respectively. β_1 and β_2 are phase constant in free space (air) and solid material (assuming z = 0). From the continuity of tangential electric field across the interface z = 0, we can obtain the equation as:

$$E_{0i}e^{-j\beta_1 x\sin\theta_i} + E_{0r}e^{-j\beta_1 x\sin\theta_r} = E_{0t}e^{-j\beta_2 x\sin\theta_t} \quad (4)$$

The phase constant in each medium is balanced. The angle of reflection is equal to the angle of Incidence, according to Snell's law of reflection, θ_i=θ_r [16].

$$\mathrm{H}_1 = \frac{1}{\eta_1}\begin{bmatrix}\mathrm{E}_{0i}(-\cos\theta_i\boldsymbol{a}_x+\sin\theta_i\boldsymbol{a}_z)e^{-j\beta_1(z\cos\theta_i+x\cos\theta_i)} \\ +\mathrm{E}_{0r}(\cos\theta_i\,\boldsymbol{a}_x+\sin\theta_i\boldsymbol{a}_z)e^{-j\beta_1(-z\cos\theta_i+x\cos\theta_i)}\end{bmatrix} \quad (5)$$

$$\mathrm{H}_2 = \frac{1}{\eta_2}\mathrm{E}_{0t}(-\cos\theta_t\boldsymbol{a}_x+\sin\theta_t\boldsymbol{a}_z)e^{-j\beta_2(z\cos\theta_t+x\cos\theta_t)} \quad (6)$$

Equations (5) and (6) showing the equation of magnetic field (H) for the Perpendicular polarized plane. Where $\eta_1$and η_2 are wave number of free space (air) and solid material (assuming z = 0). From the continuity of tangential electric field across the interface z = 0, In the case of a perpendicular polarized plane, the reflection coefficient is stated as:

$$\Gamma_\perp = \frac{\eta_2/\cos\theta_t - \eta_1/\cos\theta_i}{\eta_2/\cos\theta_t + \eta_1/\cos\theta_i} \quad (7)$$

Referring to Snell's law of refraction, the incident wave, the refracted wave, and the normal to the interface all lie in the same plane, $n_1\sin\theta_i = n_1\,sin\theta_t$ where $n_1 = \sqrt{\mu_{r1}\epsilon_{r1}}$ and $n_2 = \sqrt{\mu_{r2}\epsilon_{r2}}$ [17, 18]. From Equation 7 we can know the value of Brewster angle (θ_B), that is angle of incident where there is no reflection $\Gamma = 0$ [19].

$$Sin^2\theta_{B\perp} = \frac{1-\frac{\mu_1\epsilon_2}{\mu_2\epsilon_1}}{1-(\mu_1\mu_2)^2} \quad (8)$$

Wedges Geometry Effect on Multiple Reflections and Absorption of Electromagnetic Wave

The multi-wedges configuration in an anechoic chamber room causes each wedge to receive a different incidence wave angle based on the direction of the wave source. Wedge geometries produce many reflections towards the wedge apex like tetrahedron or pyramid geometries. Due to the angle between the direction of electromagnetic wave propagation and the surface normal, wedge surfaces provide greater reflection than flat surfaces as a natural result of Snell's law. A loss of electromagnetic wave energy is obtained by repeated reflection at the angle of the gap between the wedges before being scattered back outwards. This can be referred to as wave absorption, the value of energy absorbed for a single reflection can be given as:

$$A = \frac{1}{2}\sigma E^2 + \frac{1}{2}\omega\varepsilon_0\varepsilon_R E^2 + \frac{1}{2}\omega\mu_0\mu_R H^2 \quad (9)$$

where A (W/m^3) is electromagnetic wave absorption per unit volume, the energy absorbed by the wedge material is a form of magnetic loss and converts that energy into heat [20]. Wedge slices with narrower apex angles provide more reflection than wedges with wider apex angles, resulting in optimal absorption of electromagnetic waves. To identify the effect of the apex angle of the wedges, a test was carried out with variations in the angle of the incident wave (θ) ranging from 0°-85° with a stepping distance is 5°. It can be illustrated in Figure 2.

The low angle condition such as 0° represents that the waves coming vertically towards the top of wedges, this condition allows obtaining maximum absorption because the conductive foam can directly absorb the waves. Whereas the high angle such as 85° likely will reflect the incident waves into the air. From this possibility shows the importance of anechoic shape, so the accurate design can direct precisely the waves into the conductive foam to obtain a maximum absorption and minimal wave reflection [21].

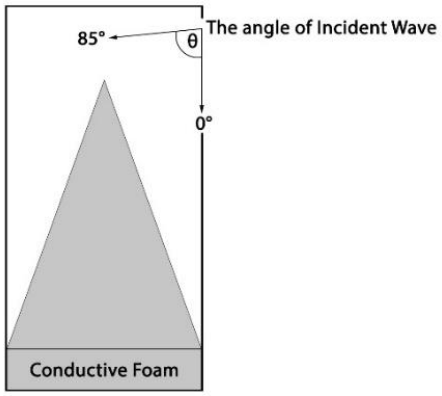

Figure 2. The Angle of Incident Wave

Wedges Model and Limitation

Model Eckel wedge structures were chosen for wedge design commonly used to implement an anechoic chamber room (i.e Microsoft anechoic chamber room, TU Delft Anechoic Chamber, etc.). According to Snell's law, the optimal absorption of sound waves is obtained when the wave reflection conditions are getting higher. Hence, studies to produce a better performance of wave reflections were carried out until now. Optimization can be attained by designing a new design, determining the slope, height, size, type of material, and distance between the wedges [22, 23, 24]. Variations models tested in this study are shown in Figure 3.

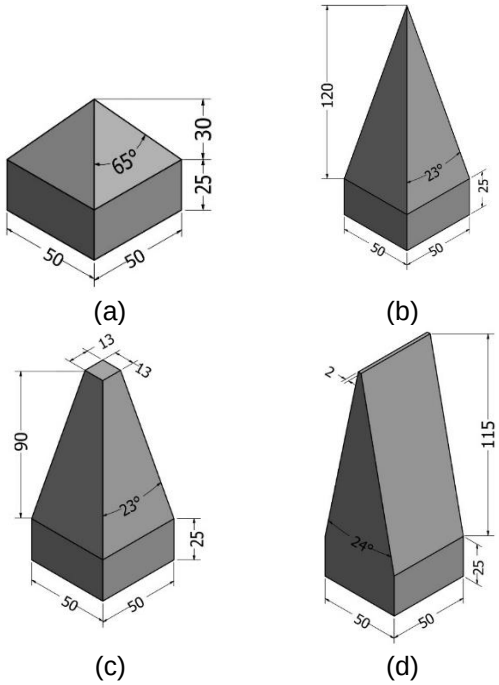

Figure 3. Various of model wedges anechoic chamber (a) Diamond, (b) Pyramidal, (c) Oblique pyramidal, and (d) Eckel

In the implementation, wedges of the anechoic chamber will be fabricated using open-cell polyurethane foam, the acoustic design is adjusted to the absorption parameters based on the ASTM C423-17 standard [25, 26].

Materials with less density generally affect the reduced cut-off frequency for the chamber and lower pressure reflection coefficient [27]. Furthermore, the type of material affects the degree of electromagnetic roughness of a surface [28].

The performance is evaluated using a frequency range of 1-3GHz. It aims to determine the performance in each frequency range and to know the design of anechoic chamber for a suitable and affordable solution based on frequency requirements. Anechoic room is considered as free field space. Hence, magnetic permeability is assumed as $\mu = \mu_0 = 4\pi\ x\ 10^{-7}\ H/m$ for the lossy dielectric material.

RESULTS AND DISCUSSION

In this work, electromagnetic wave absorption performance was tested and compared with the results of commercial models of wedges, as shown in Figure 3. The simulation process uses the COMSOL Multiphysics Software simulator. This work uses the physics interface setting of "electromagnetic wave, frequency domain" which the finite element method solves. The results obtained for testing each model are S-Parameter (dB) as a wave parameter reflectivity and electric field in the space around the wedges model to represent the distribution and pressure of the electromagnetic field.

This research is based on a computational investigation where real experiments are not carried out, the data results are validated through using the acoustic equations and setting of environmental simulation conditions. The Standard of the equations and limitations of simulation has been determined by COMSOL.

Conductive foam is used as the base material for wedges to produce optimal absorption of electromagnetic waves, has the same dimensions as the base on all models of 50 mm x 50 mm. The height of the port to the base of wedges is 165 mm. These simulation results for each model are evaluated based on the different incidence angles and range frequency, in which the incidence angle is used in the range of 0°-85° and at a frequency of 1-3 GHz.

In the 1 GHz frequency test, Eckel model obtained the best performance within the S-parameter -66.6 dB at an elevation angle of 0 rad, in the testing of elevation angle 0.4 rad, the fluctuating value is similar with pyramidal and oblique pyramidal model with the S-parameter is

around -26.6 dB. The lowest performance occurs in the diamond model with only an S-Parameter value of -5.9 dB, as shown in Figure 4.

The Eckel model conditions get a degraded performance due to geometric factors, its shape with only two beveled sides makes it produce maximum absorption performance at low angles of incidence waves, this means the wave is coming directly from the front of the anechoic chambers. However, when the waves come from the side position will reflect waves precisely into the air, it causes the absorption performance is not effective. In the setup of fixed conditions without multi-test sound sources, the best configuration of the Eckel model can be determined.

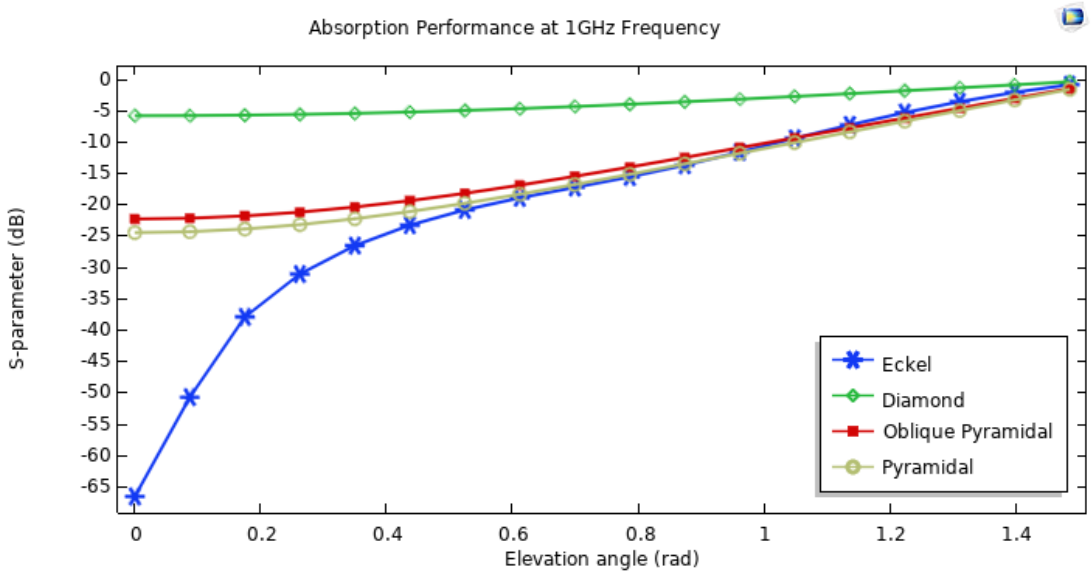

Figure 4. Comparison of various wedges model absorption performance for 1 GHz frequency

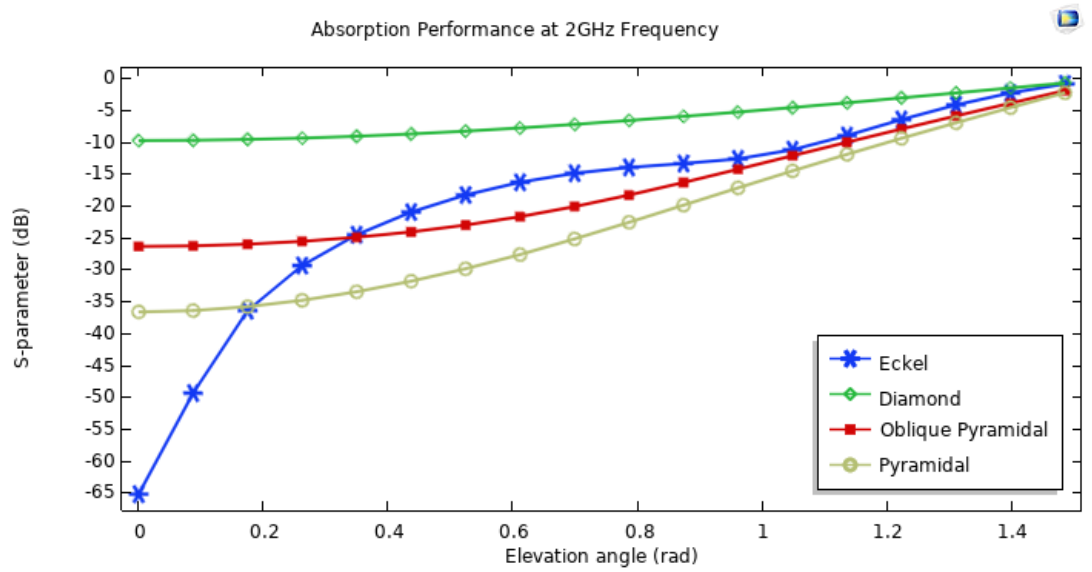

Figure 5. Comparison of various wedges model absorption performance for 2 GHz frequency

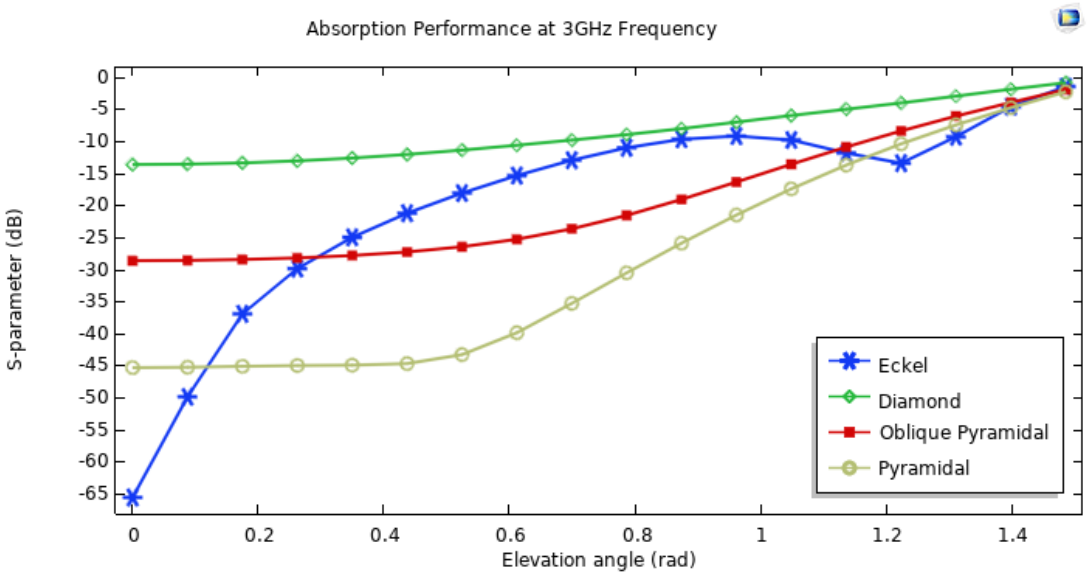

Figure 6. Comparison of various wedges model absorption performance for 3 GHz frequency

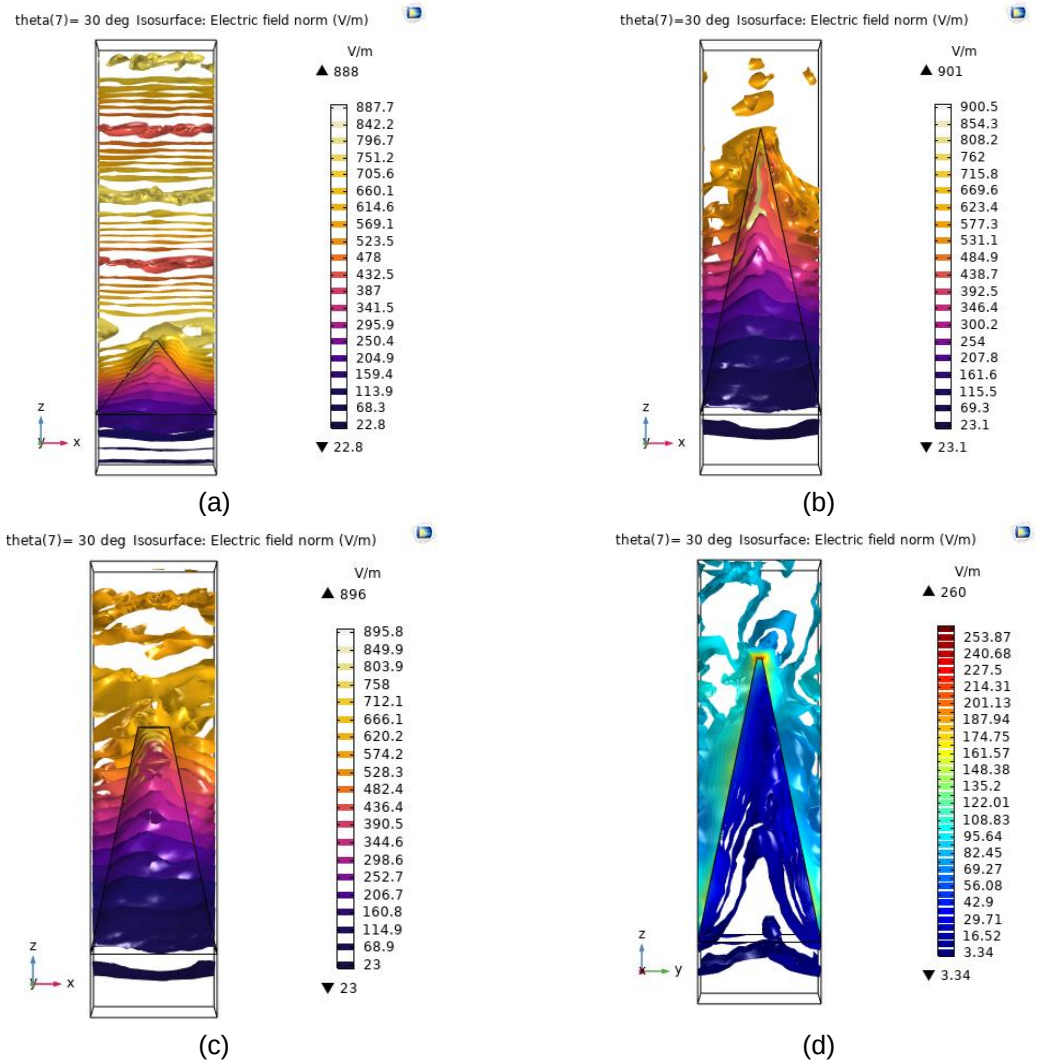

(a) (b)

(c) (d)

Figure 7. The power flow and norm of electric field where the elevation angle of incidence is 30 degrees at 3 GHz frequency: (a) Eckel, (b) Diamond, (c) Oblique pyramidal, and (d) Pyramidal

The Eckel model gets high-performance fluctuations, the best absorption performance limit occurs at a maximum elevation angle of 0.2 rad. Similar results were also found in testing at 2 GHz and 3 GHz frequencies. Meanwhile, the pyramidal model gets better results than the oblique pyramidal in these two tests. The diamond model still gets the lowest absorption performance on all ranges of the tests. Test results at 2 GHz and 3 GHz are shown in Figure 5 and Figure 6.

The geometry factor of each wedges model has a significant impact on absorption performance. The sharper Apex Angle provides better performance, as shown by comparing the oblique pyramidal model and the pyramidal model, where the pyramidal model gets better results. The formation angle in the pyramidal models of 24° gives different significant results with the diamond model which uses an angle of 65°, which causes the apex angle to be even greater. Hence, the geometry wedged with a height and a narrower apex angle will produce a good surface slope to produce optimal absorption performance. The test results are also following Snell's law, the optimal absorption of sound waves occurs when the wave reflection conditions are getting higher. in the 3 GHz frequency test, the performance of the wedge was better than other tests.

Power flow and norm of electric field are also illustrated in Figure 7. The representative of the test was carried out at 3 GHz frequency where the elevation angle of incidence is 30 degrees, and the azimuthal angle is zero. The pyramidal model gets the highest electric field norm value of 901 V/m. Other models show minor differences except for the Eckel model, which is only 260 V/m due to the effect of limited free air space and the design that only has two beveled sides.

The value of the power flux and norm of electric field describes how much of waves through the wedges. The pyramidal model obtains the best value because of the effect of using a sharp apex angle and their four beveled sides, this condition creates a good wave reflection capability between the wedges, so the waves can be optimally absorbed in the conductive foam with a minimum value of the reflected waves back into the air.

CONCLUSION

This study shows that the geometrical model on wedges anechoic chamber has a great effect on absorption performance. For instrument testing implementations with a band frequency less than or equal to 1 GHz, the Eckel model performs best due to its high absorption rate. However, the application of the Eckel model at high frequency results in a fairly fluctuating value and a decrease in performance. In implementing instrument testing with high-frequency waves, the best performance is obtained by the pyramidal model, this model produces a stable absorption value at each frequency test.

To obtain maximum absorption, it can be made by reducing the apex angle in the anechoic wedge design, using high absorption coefficient materials, and the possibility of adding beveled sides to the wedges which can have a positive impact, especially to maximize the direction of the waves for absorption and minimize the reflected waves back into the air.

In general, a pyramidal model can be an ideal absorber for anechoic applications because it provides good absorption performance for near normal and normal incidence angles. Furthermore, it can contribute positively to instrument microphone tuning and reduced antenna measurement error. This research is based on a computational study, and experimental analysis is not discussed in this work.

REFERENCES

[1] M. Amirul, A. Mohd, A. Sapit, M. A. Razali, and A. R. Saleman, "Aeroacoustic Sound Generation of Square Cylinder with Detached Flat Plate in Semi-Anechoic Chamber," *Journal of Complex Flow*, vol. 1, no. 2, pp. 1–5, 2019.

[2] A. D. Firmanto, I. Stefanus, R. Ikhwanuddin, and M. I. Mandasari, “Desain Perekaman Basis Data Suara Ucap untuk Pengembangan Sistem Rekognisi Pengucap Otomatis Forensik Berbahasa Indonesia,” *Center for open science,* 2019, doi: 10.31227/osf.io/v8ekm.

[3] T. Sheret, and B. Allen, "Calibration of An Anechoic Chamber for Measurement of a Multi-Channel Antenna," *Research Report*, The University of Bedfordshire. 2014.

[4] M. A. K. Wiles, and A. Kriz, "Multi-Purpose Anechoic Chambers - EMC (SAR / FAR) to Antenna Measurements," *Research Report*, Seibersdorf Laboratories. 2005.

[5] M. Amiri, F. Tofigh, N. Shariati, J. Lipman, and M. Abolhasan, “Wide-angle metamaterial absorber with highly insensitive absorption for TE and TM modes,” *Nature-research Scientific Reports*, vol. 10, no. 1, pp. 1–13, 2020, doi: 10.1038/s41598-020-70519-8.

[6] NN, “ISO 3745 Acoustics, Determination of Sound Power Levels of Noise Sources Using Sound Pressure—Precision Methods for Anechoic and Hemi-anechoic Rooms,” *International Organization for Standardization*, Geneva, Switzerland, 2003.

[7] R. Kapoor, N. Kloet, A. Gardi, A. Mohamed, and R. Sabatini, “Sound propagation modelling for manned and unmanned aircraft noise assessment and mitigation: A review,” *Atmosphere (Basel)*, vol. 12, no. 11, pp. 1–21, 2021, doi: 10.3390/atmos12111424.
[8] R. Rusz, "Design of a Fully Anechoic Chamber", *Master Thesis,* KTH Engineering Sciences. 2015.
[9] C. Jiang, S. Zhang, and L. Huang, "On the acoustic wedge design and simulation of anechoic chamber," *Journal of Sound and Vibration*, vol. 381, pp. 139–155, 2016, doi: 10.1016/j.jsv.2016.06.020.
[10] L. M. Kasim et al., “A Study of Electromagnetic Absorption Performance of Modern Biomass Wall Tile,” *International Journal of Electrical and Electronic Engineering and Telecommunications*, vol. 9, no. 6, pp. 429–433, 2020, doi: 10.18178/IJEETC.9.6.429-433.
[11] I. Catalkaya and S. Kent, "Analysis of multiple wedges electromagnetic wave absorbers," *Progress in Electromagnetics Research*, vol. 26, pp. 1-9, 2012, doi: 10.2528/ PIERM12071204.
[12] G. Fusaro, F. D’Alessandro, G. Baldinelli, and J. Kang, “Design of urban furniture to enhance the soundscape: A case study,” *Building Acoustics*, vol. 25, no. 1, pp. 61–75, 2018, doi: 10.1177/1351010X18757413.
[13] M. Russo, L. Kraljević, M. Stella, and M. Sikora, “Acoustic performance analysis of anechoic chambers based on ISO 3745 and ISO 26101: standards comparison and performance analysis of the anechoic chamber at the University of Split,” *Proceedings of Euronoise 2018*, pp. 2225–2230, 2018.
[14] M. Al Zubi, “Measurement of Sound Pressure Levels in Anechoic Chamber and a Noisy Environment Experimentally,” *Open Journal of Acoustics*, vol. 08, no. 02, pp. 13–22, 2018, doi: 10.4236/oja.2018.82002.
[15] S. Rao Singeresu, *The Finite Element Method in Engineering*, Butterworth-Heinemann Elsevier, Amsterdam, Dutch, 2018.
[16] A. Ishimaru, *Electromagnetic Wave Propagation, Radiation, and Scattering,* John Wiley & Sons, Inc. Canada. 2017.
[17] D. K. Cheng, *Field and Wave Electromagnetics*, 2nd Edition. Pearson Education: Addison-Wesley, 1989.
[18] A. Langenbucher, *Law of Refraction (Snell’s Law) BT - Encyclopedia of Ophthalmology*. Berlin, Heidelberg: Springer Berlin Heidelberg, 2018.
[19] T. Abuelfadl, "Refection and Transmission," Electronics and Electrical Communications Department. Cairo University. 2018.
[20] M. Jaroszewski, S. Thomas, and A. V. Rane, *Advanced Materials for Electromagnetic Shielding*. John Wiley & Sons, Inc. Hoboken. 2019.
[21] P. Pinho, H. Santos, and H. Salgado, “Design of an anechoic chamber for w-band and mm-wave,” *Electronics*, vol. 9, no. 5, pp. 1-13, 2020, doi: 10.3390/electronics9050804.
[22] V. Rodriguez, “Validation of a Method for Predicting Anechoic Chamber Performance: A Technique That Uses Polynomial Approximations for RF Absorber Reflectivity,” *IEEE Antennas Propagation Magazine.*, vol. 60, no. 4, pp. 31–40, 2018, doi: 10.1109/MAP.2018.2839895.
[23] D. Fan, “Electromagnetic Anechoic Chamber Design and Optimization Method,” *International Conference on Microwave and Millimeter Wave Technology.* pp. 1–3, 2019, doi: 10.1109/ICMMT45702.2019.8992879.
[24] J. Luis, E. Cuello, J. Fernando, and P. Ospina, “Low-cost and easily implemented anechoic acoustic chambers,” *Scientia et Tecnica Año XXIII*, vol. 23, no. 4, pp. 471–478, 2018, doi: 10.22517/23447214.18421.
[25] S. Zhang and J. Lee, “Diffuseness quantification in a reverberation chamber and its variation with fine-resolution measurements,” *Buildings*, vol. 11, no. 11, 2021, doi: 10.3390/buildings11110519.
[26] ASTM International, ASTM C423-17, “*In Standard Test Method for Sound Absorption and Sound Absorption Coefficients by the Reverberation Room Method”*, ASTM International: West Conshohocken, PA, USA, 2017.
[27] S. K. Sushil, M. Garg, and S. Narayanan, “Estimation of the lower cut-off frequency of an anechoic chamber: An empirical approach,” *International Journal of Aeroacoustics*, vol. 19, no. 1–2, pp. 57–72, 2020, doi: 10.1177/1475472X20905070.
[28] Z. Cai *et al.*, “Small Anechoic Chamber Design Method for On-Line and On-Site Passive Intermodulation Measurement,” *IEEE Transactions on Instrumentation and Measurement*, vol. 69, no. 6, pp. 3377–3387, 2020, doi: 10.1109/TIM.2019.2937425.